

3,5-Dimethyl-1,3,5-oxadiazane-2,4,6-trione: short intermolecular contacts determining the crystal packing

Janna Geith, Thomas M. Klapötke, Peter Mayer, Axel Schulz and Jan J. Weigand*

Department Chemie und Pharmazie, Ludwig-Maximilians Universität, Butenandtstraße 5-13 (Haus D), D-81377 München, Germany
Correspondence e-mail: jan.weigand@cup.uni-muenchen.de

Received 4 March 2005
Accepted 21 July 2005
Online 10 August 2005

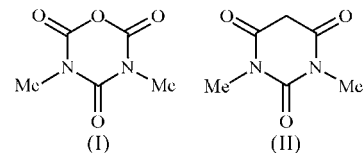
In the title compound, $C_5H_6N_2O_4$, the molecules lie across a crystallographic mirror plane. The compound lacks traditional hydrogen-bond donors, and hence crystals are held together by unusual $C=O \cdots O$, $O \cdots C$ and weak $C-H \cdots O$ interactions, forming layers. Adjacent layers are arranged in an antiparallel manner, yielding an *ABA* layer sequence. The intermolecular contacts are quite short; a topological analysis of charge density based on density-functional-theory calculations was used for consideration of these short contacts and indicated a strong attractive bonding closed-shell interaction between these atoms in the crystal structure.

Comment

Intermolecular interactions are the basis for crystal engineering, their nature and strength determining their competitive importance in forming different crystal packings (Desiraju, 1995). Among these intermolecular forces, hydrogen bonds are the most important in view of their higher energy and directionality. The three-dimensional network in a crystal is also determined by other forces, such as multipolar electrostatic, donor–acceptor and van der Waals interactions (Dunitz, 1996). For the consideration of non-bonded interactions, for a long time, the van der Waals radii concept (Bondi, 1964; Zefirov & Zorky, 1989) has been a common approach, but more recently, mean statistical contacts (Rowland & Taylor, 1996) have also been suggested for this purpose. There is a somewhat arbitrary dividing line between what is or is not an interaction, and none of these approaches give a valid conclusion about the nature of these short contacts; furthermore, in general, attractive and repulsive interactions cannot be distinguished.

The structure of the molecule of the title compound, (I), is shown in Fig. 1. The molecule is a cyclic derivative of urea, containing an anhydride moiety. X-ray investigation has shown that the bond lengths in (I) do not differ considerably from standard values found in other anhydrides, as well as

urea derivatives (Bolte & Bauch, 1999), and the structure is related to 1,3-dimethylbarbituric acid, (II), where the CH_2 fragment is replaced by an O atom (Bertolasi *et al.*, 2001). The molecule of (I) lies across a crystallographic mirror plane passing through atoms O1, O3 and C2. Geometric parameters are given in Table 1.



The smallest subunit of the packing mode in (I) consists of a trimer arrangement of molecules, as shown in Fig. 2. Because (I) does not have traditional hydrogen-bond donor groups, molecules interact in the crystal by means of unusual short $C=O \cdots O$ and $O \cdots C$ contacts, and weak $C-H \cdots O$ hydrogen bonds. The units are linked into chains by a very short $C=O \cdots O$ [$O1 \cdots O3^{ii} = 2.842(3) \text{ \AA}$; symmetry code: (ii) $x - \frac{1}{2}, -y + \frac{1}{2}, -z + \frac{3}{2}$] interaction. These chains are, in turn, transformed into layers by further short contacts [$C=O3 \cdots O1^{iii} = 3.106(2) \text{ \AA}$ and $O1^{iii} \cdots C2^{ii} = 3.257(2) \text{ \AA}$; symmetry code: (iii) $x, y, z - 1$] and weak $H3 \cdots O2^{iii}$ and

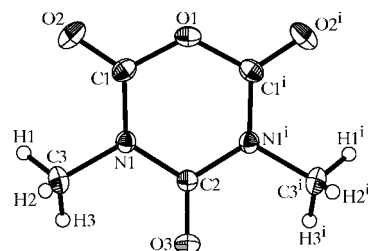


Figure 1

A view of the molecular structure of (I), showing the atom-labeling scheme. Displacement ellipsoids are drawn at the 50% probability level and H atoms are shown as small spheres of arbitrary radii. [Symmetry code: (i) $x, -y + \frac{1}{2}, z$.]

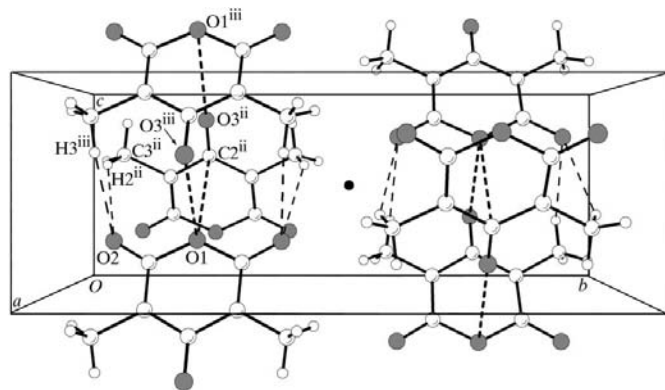


Figure 2

The molecular packing in (I), shown in a perspective view along the *a* axis. Thick dashed lines represent $C=O \cdots O$ and $C \cdots O$ closed-shell bonding contacts, while thin dashed lines represent $C-H \cdots O$ hydrogen bonds. The dot indicates the inversion center located in the middle of the unit cell. [Symmetry codes: (ii) $x - \frac{1}{2}, -y + \frac{1}{2}, -z + \frac{3}{2}$; (iii) $x, y, z - 1$.]

$\text{H}2^{\text{ii}} \cdots \text{O}2^{\text{iii}}$ hydrogen bonds, having distances of 2.78 (2) and 2.58 (3) Å, respectively. The three contacts are comparable to the sum of the C and O van der Waals radii, of 3.04 (O + O) and 3.22 Å (C + O; Bondi, 1964), and are to be compared with an average of *ca* 3.4 Å and a minimum of 2.8 Å found for comparable types of interactions (Allen *et al.*, 1998; Zacharias & Glusker, 1984). Adjacent layers are arranged in a reverse manner and there are no particularly strong interactions between these layers, indicating a simple close packing. The lateral packing of the layers arranged in an antiparallel manner (*ABA* layer sequence) is simply a consequence of the centrosymmetric nature of the space group *Pnma*.

The theory of atoms in molecules (Bader, 1990) can be used to analyze the chemical bonding in terms of shared (covalent) and closed-shell interaction (van der Waals, ionic bonding, *etc.*) with respect to the attractive bonding character of short contacts. This theory describes a molecule in terms of electron density, $\rho(r)$, its gradient vector field, $\nabla\rho(r)$, Laplacian, $\nabla^2\rho(r)$, and bond critical points, CP. The type of interaction is characterized by the sign and magnitude of the Laplacian $\rho(r_b)$ at the bond critical point. If electronic charge is concentrated in the bond CP [$\nabla^2\rho(r_b) < 0$], this type of interaction is referred to as a shared interaction. Interactions that are dominated by contraction of charge away from the interatomic surface toward each nuclei [$\nabla^2\rho(r_b) > 0$] are called closed-shell interactions. For closed-shell interactions, $\rho(r_b)$ is relatively low in value, and the value of $\nabla^2\rho(r_b)$ is positive. The sign of the Laplacian is determined by the positive curvature of $\rho(r_b)$ along the interaction line, as the exclusion principle leads to relative depletion of charge in the atomic surface. Critical points of the (3, -1) type, so-called bond critical points, provide, according to Bader (1990), a universal indicator of bonding between these atoms and are of prime importance from the chemical standpoint. It is believed that a bonding interaction occurs between the atoms if there is

a line (bonding path) linking their nuclei along which the charge density has a maximum with respect to any lateral shift and which has a minimum at the bond critical point (3, -1).

The trimer unit as shown in Fig. 2 was used for the analysis of the intermolecular interactions in (I), and every expected covalent bond has been characterized by a negative Laplacian at the bond CP. In addition to the expected path network, three (3, -1) unusual bond CPs have been found on the $\text{O}1 \cdots \text{O}3^{\text{ii}}$ (CP1), $\text{O}3 \cdots \text{O}1^{\text{iii}}$ (CP2) and $\text{O}1^{\text{iii}} \cdots \text{C}2^{\text{ii}}$ (CP3) lines (Table 2). Fig. 3 (left) shows the gradient lines of the electron density and the projection of the molecular graph on to the mirror plane $\text{O}1 \cdots \text{O}1^{\text{iii}} \cdots \text{C}2^{\text{ii}}$ containing CP1, CP2 and CP3. In Fig. 3 (right), a few of the gradient lines and the projection of the molecular graph on to $\text{O}1 \cdots \text{O}3^{\text{ii}} \cdots \text{C}3^{\text{ii}}$ show the origin of the strongest attractive interaction between atoms O1 and $\text{O}3^{\text{ii}}$ (CP1).

The calculated positive Laplacian of the electron density [$\nabla^2\rho(r_b)$] and the relatively low value of $\rho(r_b)$ at the bond critical points (Table 2) indicate that the closest $\text{O}1 \cdots \text{O}3^{\text{ii}}$ (CP1), $\text{O}3 \cdots \text{O}1^{\text{iii}}$ (CP2) and $\text{O}1^{\text{iii}} \cdots \text{C}2^{\text{ii}}$ (CP3) contacts (Klapötke *et al.*, 2005), as well as the weak hydrogen bonds $\text{H}2^{\text{ii}} \cdots \text{O}2^{\text{iii}}$ (CP4) and $\text{H}3 \cdots \text{O}2^{\text{iii}}$ (CP5), are dominated by closed-shell interactions. The high values of the ratio $G(r_b)/\rho(r_b)$ at the bond CPs (Table 2) and the ratio of the eigenvalues $|\lambda_1|\lambda_3 \ll 1$ support this conclusion (Table 3; Bader & Essen, 1984). Additional information about chemical bond types is available from total electronic energy density $Ee(r_b) = G(r_b) + V(r_b)$. Closed-shell interactions are dominated by the kinetic energy density, $G(r_b)$, in the region of the bond CP, with $G(r_b)$ being slightly greater than the potential energy density $|V(r_b)|$ and with the energy density [$Ee(r_b) > 0$] close to zero (Table 2).

The values found for $\rho(r)$ in (I) at the critical points for intermolecular C—H \cdots O contacts (CP4 and CP5; Table 2) are comparable to those reported for intermolecular hydrogen bonds studied previously (Koch & Popelier, 1995).

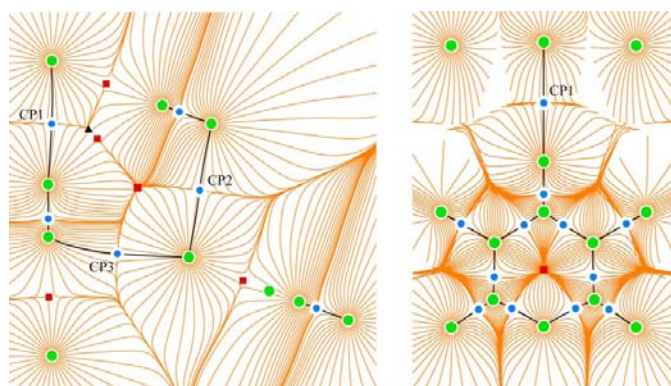


Figure 3

Left: gradient lines of the electron density and the projection density of the molecular graph on to the $\text{O}1 \cdots \text{O}1^{\text{iii}} \cdots \text{C}2^{\text{ii}}$ plane. Right: gradient lines of the electron density and the projection density of the molecular graph on to the $\text{O}1 \cdots \text{O}3^{\text{ii}} \cdots \text{C}3^{\text{ii}}$ plane. Each line represents a trajectory of $\nabla\rho$, which is a line of steepest ascent through the charge density. Most trajectories are attracted to a nucleus and constitute an atomic basin. The bond CPs are shown as circles, the ring CPs as rectangles and the cage critical point as triangles.

Experimental

To a cooled (268 K) suspension of dry *N,N'*-dimethylurea (5.57 mmol) in MeCN (20 ml) was added slowly chlorosulfonyl-isocyanate (9.8 ml, 114 mmol) under nitrogen. The solution was stirred for 4 h at room temperature and quenched with ice (80 g). The reaction mixture was reduced to one-third of its volume and cooled at 278 K overnight. The resulting colorless powder was recrystallized from acetone, yielding (I) as colorless rods suitable for single-crystal X-ray diffraction (m.p. 524 K). IR (cm^{-1}): 1832 (C=O), 1766 (C=O), 1708 (C=O); ^1H NMR ($[d_6]$ -DMSO): δ 3.16 (3H, s); ^{13}C NMR ($[d_6]$ -DMSO): δ 29.5 (CH_3), 144.7 (C), 148.6 (C).

Crystal data

$\text{C}_5\text{H}_6\text{N}_2\text{O}_4$
 $M_r = 158.11$
 Orthorhombic, *Pnma*
 $a = 7.7406$ (7) Å
 $b = 14.9682$ (14) Å
 $c = 5.4928$ (7) Å
 $V = 636.41$ (12) Å³
 $Z = 4$
 $D_x = 1.650$ Mg m⁻³

Mo $K\alpha$ radiation
 Cell parameters from 3141 reflections
 $\theta = 2.7$ – 28.0°
 $\mu = 0.15$ mm⁻¹
 $T = 200$ (2) K
 Rod, colorless
 $0.42 \times 0.15 \times 0.09$ mm

Data collection

Stoe IPDS diffractometer	$R_{\text{int}} = 0.048$
φ or ω scans	$\theta_{\text{max}} = 28.0^\circ$
5084 measured reflections	$h = -10 \rightarrow 9$
794 independent reflections	$k = -18 \rightarrow 19$
595 reflections with $I > 2\sigma(I)$	$l = -7 \rightarrow 7$

Refinement

Refinement on F^2	All H-atom parameters refined
$R[F^2 > 2\sigma(F^2)] = 0.033$	$w = 1/[\sigma^2(F_o^2) + (0.0647P)^2]$
$wR(F^2) = 0.092$	where $P = (F_o^2 + 2F_c^2)/3$
$S = 0.96$	$(\Delta/\sigma)_{\text{max}} < 0.001$
794 reflections	$\Delta\rho_{\text{max}} = 0.18 \text{ e } \text{\AA}^{-3}$
67 parameters	$\Delta\rho_{\text{min}} = -0.21 \text{ e } \text{\AA}^{-3}$

Table 1

Selected geometric parameters (\AA , $^\circ$).

O1—C1	1.3658 (13)	N1—C1	1.3587 (14)
O2—C1	1.1919 (15)	N1—C2	1.3798 (12)
O3—C2	1.2008 (18)	N1—C3	1.4669 (15)
C1—O1—C1 ⁱ	123.95 (12)	O2—C1—O1	118.61 (11)
C1—N1—C2	123.55 (10)	N1—C1—O1	116.38 (10)
C1—N1—C3	118.29 (10)	O3—C2—N1	122.03 (6)
C2—N1—C3	118.14 (10)	N1 ⁱ —C2—N1	115.93 (13)
O2—C1—N1	125.01 (12)		

Symmetry code: (i) $x, -y + \frac{1}{2}, z$.

Table 2

Bond critical points in (I).

CP	$\rho(r_b)$	$\nabla^2\rho(r_b)$	$G(r_b)$	$V(r_b)$	$G(r_b)/\rho(r_b)$	ϵ
CP1	0.0103	0.0443	0.0095	-0.0079	0.920	0.5635
CP2	0.0062	0.0219	0.0049	-0.0043	0.784	0.0133
CP3	0.0042	0.0184	0.0035	-0.0024	0.830	2.5156
CP4	0.0073	0.0273	0.0056	-0.0045	0.776	0.1372
CP5	0.0046	0.0163	0.0034	-0.0027	0.732	0.0663

Notes: all quantities in atomic units; CP is a (3, -1) critical point, ρ is electron density, $\nabla^2\rho$ is the Laplacian of ρ , G is the kinetic and V the potential energy density, and ϵ is the ellipticity; B3LYP/6-311+G(3d,2p) density; X-ray structural data used.

Table 3

Eigenvalues.

CP	λ_1	λ_2	λ_3	$ \lambda_1/\lambda_3 $
CP1	-0.0081	-0.0052	0.0577	0.141
CP2	-0.0048	-0.0048	0.0315	0.154
CP3	-0.0022	-0.0006	0.0213	0.104
CP4	-0.0068	-0.0060	0.0401	0.171
CP5	-0.0040	-0.0038	0.0240	0.167

Note: $\lambda_{1,2,3}$ are eigenvalues of the Hessian of ρ .

All non-H atoms were refined with anisotropic displacement parameters, employing a rigid-bond restraint to U^{ij} of the two bonded atoms (Rollett, 1970). The quantum-chemical calculations for (I)

were performed at the B3LYP/6-311+G(3d,2p) level using the GAUSSIAN98 package (Frisch *et al.*, 1998). Single-point calculations at the experimental geometry of a subunit of the crystal structure were performed, with no geometry optimization. Wavefunction files suitable for direct reading by AIM2000 (Biegler-Koenig, 2002) were obtained using the 'output = wfn' option. The topological analysis of the theoretical charge-density distribution was carried out using AIM2000.

Data collection: IPDS Software (Stoe & Cie, 1997); cell refinement: IPDS Software; data reduction: IPDS Software; program(s) used to solve structure: SHELXS97 (Sheldrick, 1997); program(s) used to refine structure: SHELXL97 (Sheldrick, 1997); molecular graphics: DIAMOND (Brandenburg, 2000); software used to prepare material for publication: SHELXL97.

Financial support of this work by the University of Munich (LMU) and the Fonds der Chemischen Industrie is gratefully acknowledged (JJW acknowledges an FCI scholarship, DO 171/46). The authors also thank the Leibniz Rechenzentrum for a generous allocation of CPU time.

Supplementary data for this paper are available from the IUCr electronic archives (Reference: FR1522). Services for accessing these data are described at the back of the journal.

References

Allen, F. H., Baalham, C. A., Lommerse, J. P. M. & Raithby, P. R. (1998). *Acta Cryst.* **B54**, 320–329.

Bader, R. F. W. (1990). *Atoms in Molecules: A Quantum Theory*. New York: Oxford University Press.

Bader, R. F. W. & Essen, H. (1984). *J. Chem. Phys.* **80**, 1943–1960.

Bertolasi, V., Gilli, P., Ferretti, V. & Gilli, G. (2001). *New J. Chem.* **25**, 408–415.

Biegler-Koenig, F. W. (2002). *AIM2000*. Version 2.0. University of Applied Science, Bielefeld, Germany.

Bolte, M. & Bauch, C. (1999). *Acta Cryst.* **C55**, 226–228.

Bondi, A. (1964). *J. Phys. Chem.* **68**, 441–451.

Brandenburg, K. (2000). *DIAMOND*. Version 2.1.e. Crystal Impact GbR, Bonn, Germany.

Desiraju, G. R. (1995). *Angew. Chem. Int. Ed. Engl.* **34**, 2311–2327.

Dunitz, J. D. (1996). *The Crystal as a Supramolecular Entity*, edited by G. R. Desiraju, ch. 1, pp. 1–78. Chichester: John Wiley and Sons.

Frisch, M. J., Trucks, G. W., Schlegel, H. B., Scuseria, G. E., Robb, M. A., Cheeseman, J. R., Zakrzewski, V. G., Montgomery, J. A. Jr, Stratmann, R. E., Burant, J. C., Dapprich, S., Millam, J. M., Daniels, A. D., Kudin, K. N., Strain, M. C. *et al.* (1998). *GAUSSIAN98*. Revision A11. Gaussian Inc., Pittsburgh, PA, USA.

Klapötke, T. M., Mayer, P., Schulz, A. & Weigand, J. J. (2005). *J. Am. Chem. Soc.* **127**, 2032–2033.

Koch, U. & Popelier, P. L. A. (1995). *J. Phys. Chem.* **99**, 9747–9754.

Rollett, J. S. (1970). *Crystallographic Computing*, edited by F. R. Ahmed, S. R. Hall & C. P. Huber, pp. 167–181. Copenhagen: Munksgaard.

Rowland, R. S. & Taylor, R. (1996). *J. Phys. Chem.* **100**, 7384–7391.

Sheldrick, G. M. (1997). *SHELXS97* and *SHELXL97*. University of Göttingen, Germany.

Stoe & Cie (1997). *IPDS Software*. Version 2.87. Stoe & Cie, Darmstadt, Germany.

Zacharias, D. E. & Glusker, J. P. (1984). *Acta Cryst.* **C40**, 2100–2103.

Zefirov, Yu. & Zorky, P. M. (1989). *Russ. Chem. Rev.* **58**, 713–746.